International Journal of
INTELLIGENT SYSTEMS AND APPLICATIONS IN ENGINEERING
ISSN:2147-6799 www.ijisae.org Original Research Paper

Interpretation of Change in Stress Measurement using Strain Gauge during Stressing of Pre-stressing Cables in a Bridge Span

Partha Pratim Roy[1], **Amitava Sil**[2]

Submitted: 05/02/2024 **Revised**: 13/03/2024 **Accepted**: 19/03/2024

Abstract: This paper presents a comprehensive study of the interpretation of changes in stress measurements using strain gauges during stressing of prestressed cables in a bridge span. The use of prestressed concrete in bridge construction has become prevalent owing to its ability to counteract tensile stresses and enhance structural integrity. Strain gauges are commonly employed to monitor the stress levels within the prestressing cables during the stressing process. This paper employs computer simulations to analyze and interpret the changes in stress measurements obtained from strain gauges during cable stressing, contributing to a deeper understanding of the structural behavior and load distribution. The study employs a finite element analysis (FEA) to simulate the cable stressing process, providing insights into the stress redistribution within the bridge span. The findings highlight the significance of accurate stress interpretation in ensuring the safety and efficiency of pre-stressed concrete bridge structures.

Keywords: *Stress Measurement using Strain Gauge, Stressing of Pre-stressing Cables in a Bridge Span, Simulation using Computer Models for Pre-stressing*

1. Introduction:

Prestressed concrete bridges were erected effectively worldwide during 1985 to achieve bridges with spans longer than concrete bridges. A prestressed concrete bridge is a structure in which the deflection or cracks produced are reduced by introducing pre-stress forces using prestressing tendons embedded in them. Due to some structural behavior, the prestress force introduced inside the concrete by the tendons creates a significant effect on the performance of pre-stressed concrete bridge. The pre-stress force of the pre-stressing tendons immediately experiences changes after their introduction due to not only the loss of pre-stress but due to other various factors of the lifespan of the structure like corrosion, creep, relaxation and drying shrinkage which must be managed appropriately during evaluation all throughout the service life. Pre-stressed concrete is widely used in modern bridge construction to enhance load-bearing capacity and durability. During the construction phase, pre-stressing cables are subjected to high tension forces to induce compressive stresses in the concrete. Monitoring the stress distribution within these cables is crucial to ensure the structural integrity of the bridge. Strain gauges are commonly used to measure the strains and, consequently, the stresses experienced by the cables. This paper investigates the interpretation of stress changes in pre-stressing cables using strain gauges during the stressing process, employing computer simulations to analyze the intricate behavior of these cables under varying loads.

Khandela et al. [1] studied statistical damage detection and evaluated the long-term performance of newly constructed pre-stressed concrete girders that were instrumented with fiber Bragg grating sensors. They used a framework for damage detection and localization in newly constructed prestressed concrete bridge girders using fiber optic sensing and Artificial Neural Networks (ANNs). They approached an inferred relationship between the strain profiles at different sensors distributed across the girder to detect localized damage under variable amplitude loading. The damage detection and localization approach does not require any applied loads as input parameter or detailed finite element analysis of the investigated component. In addition, it has given higher accuracy compared to other monitoring techniques relying on foil-type strain gages. Helder Sousa et al [2] estimated bridge deflection of pre-stressed concrete beam in order to appraise its performance in laboratory conditions. The evaluation of the bridge deflection based on rotation measurements, the obtained results allowed for the definition of the relative position of the inclinometers for both bridges erected using the balanced cantilever method. They found that the bridge deflections calculated using polynomial functions deviated slightly from the results obtained using the numerical model. This was because of the unsatisfactory results obtained for rotations near the support piers.

---

[1] *Research Scholar, Department of Civil Engineering, Indian Institute of Engineering Science and Technology, Shibpur, Howrah – 711103, Email : pproy76@gmail.com*

[2] *Corresponding Author, Scientist, Institute of Wood Science and Technology, Kolkata 700061, India, Email: silchief@gmail.com*

Sreeshylam et al. [3] discussed the potential of vibrating wire strain gauges for long-term monitoring of civil engineering structures. They assessed the stress condition and determined the remaining life of the structures which is important. They observed that the monitoring of civil structures requires reliable sensors that can be embedded or mounted on concrete, steel and other construction materials. The sensors should be simple to install and rugged enough to withstand harsh field conditions. Vibrating wire sensors, which are stable over long duration, are preferred for stress condition monitoring in structures. Wei-Hua Hu et al [4] had taken measurements of pre-stressed concrete bridge for 14 years' time span on variations of the strain, crack and inclination measurements. They observed crack and inclination of the bridge were strongly influenced by seasonal temperature variation. It further induces the change in relationship between the strains measured in both concrete and in the pre-stressed tendon. They proposed a health index in a framework of regression model and process control theory by investigating the linear relationship between strains in concrete and in pre-stressed tendon. The tendency of the health index during 14 years' time span may suggest the long-term bridge change during that time frame.

Wei Sun et al. [5] described a multi-point strain monitoring method which is based on distributed sensors, that can monitor the multi-point stress of pre-stressed tendons in the concrete. Firstly, the special sensor protection device is installed in the designated position of the component. The method can be applied to monitor the construction period and initial operation period of a large-span spatial structure. This method well realize the multi-point monitoring of the pre-stressed tendon strain in the concrete, and can effectively solve the engineering problems through analysis of the long-term monitoring data. They briefed that the monitoring data plays a positive role in guiding the construction of pre-stressed structure, and hence the construction safety can be objectively evaluated by analyzing the monitoring data. Junhwa Lee et al [6] demonstrated the long-term application of displacement measurement methods on full-scale railway bridge by using a dual-camera system, a light detection and ranging (LiDAR) system, strain gauge, linear variable differential transformer (LVDT), and ring gauge for long-term monitoring for around 548 days. They finally found that the displacements are analyzed based on dead loads and weather conditions, elucidating the practical issues arising in the long-term displacement monitoring of a full-scale bridge.

The geometric shape of a continuous bridge changes with variable cross-section which is due to the complex topography, strict requirement for construction as well as the significant effect arising out from stress and strain. It is always difficult to control the geometric shape of the bridge without stress monitoring system. Bin Zhou et al [7] introduced the influence of stress on construction of concrete continuous bridge. They observed that through actual monitoring, the changing speed of cantilever elevation is different under the influence of stress and the approximate law of compressive stress always exists during the process of construction. This is very much required as it contribute to the designs of the bridge conforming to the requirements and accomplish the purpose of monitoring the construction work. Ammar Zalt [8] studied the feasibility and performance of two types of sensors that has been assessed and evaluated. During short-term evaluation of these sensors, he found that both the sensors has the potential to be embedded inside concrete bridges which will be able to detect defects at their onset. The results of the accuracy test conducted on the concrete cylinders in laboratory showed an excellent agreement between the theoretical strain and the one that obtained from both sensors. Based on the same validation method, he conducted repeatability and reproducibility tests where both the sensors showed good agreements and consistent results.

Accurate interpretation of stress changes is pivotal for the design and safety of pre-stressed concrete bridges. Methodology using instrumentation is not very well verged as per Indian Standards [9], which build scope of this study. The study underscores the importance of considering stress redistribution when assessing the overall load-carrying capacity and potential weak points within the structure. R. Mani Sekhar [10] found out that by monitoring the pre stresses in concrete bridges, a clear road map can be drawn fort retrofitting or strengthening of bridges. By identifying the amount of loss of pre stress, the engineers can arrive at a judgment regarding distress condition of bridge which could also facilitate to avoid further distress in bridges. He stressed that tendons needs to periodically monitored to avoid further uncertainties of existing concrete bridges. He suggested that load cells may be attached at the end plate of post tensioned of concrete girder bridges which are to be constructed in near future to that proper monitoring of the pre stress in tendons can be carried out.

C. Robberts-Wollmann et.al [11] in their paper had presented the results of field study of different losses found in external post-tensioning tendons. They had developed an innovative system to measure strains in external tendon bundles. The system was installed on 16 tendons in an urban viaduct of segmental post-tensioned box girders. Measurements were taken to examine initial prestress losses, such as losses through stressing hardware, friction losses, seating losses, and elastic shortening losses. Measurements were recorded for over a year to study time-dependent losses. Recommendations are presented for modifications to the current methods for computing prestress losses in external tendons presented in the "American Association of State Highway and Transportation Officials (AASHTO) Guide Specification for the Design and Construction of Segmental Concrete Bridges.

This paper demonstrates the significance of accurate stress interpretation using strain gauges during the stressing of pre-stressing cables in bridge spans. Computer simulations provide valuable insights into stress redistribution and load transfer mechanisms. The findings contribute to a better understanding of the structural behavior of pre-stressed concrete bridges, enhancing their safety and efficiency during their operational lifespan.

2. Methodology

The methodology involves a comprehensive simulation-based approach utilizing finite element analysis (FEA). Computer models are developed to replicate the bridge span and pre-stressing cables. The cables are subjected to incremental loads to simulate the stressing process, and strain gauges are strategically placed to monitor the strains. The FEA software calculates the stresses based on the strains measured by the strain gauges.

3. Field Setup and Collection of data

Strain gauges will be affixed within the designated sections of the bridge spans, specifically at three distinct positions along their length: L/4, 2L/4 (equivalent to L/2), and 3L/4 (Ref Fig 1). In numerous instances, multiple instances of this configuration will be implemented along the parallel girders or on both sides of the undersurface of the deck slab. This strategic arrangement aims to optimize data collection efficiency and mitigate potential sources of interference or extraneous signals.

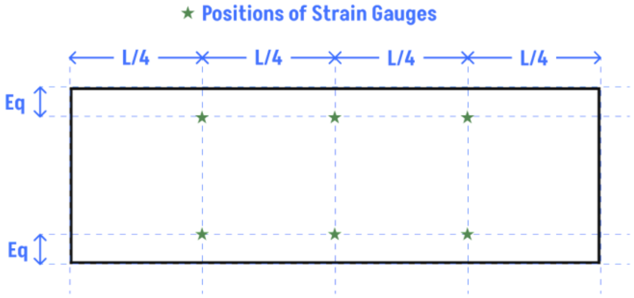

Fig. 1. Suggested position in the direction of traffic

Furthermore, the acquisition of exhaustive data concerning the bridge span is essential. This encompasses design blueprints, specifics of the pre-stressing process, material characteristics, and initial stress assessments. A representative and comprehensive enumeration of this data includes, but is not restricted to:

(a) GAD of Bridge Span under consideration

(b) Actual Comprehensive Strength of the Concrete on 28 days

(c) Actual Comprehensive Strength of the Concrete at the day of Stressing

(d) Modulus of Elasticity of the Reinforcement

(e) Yield strength of the Reinforcement Support / Bearing Details

Comprehensive details regarding the utilized pre-stressing procedure are essential, specifically emphasizing the pre-stressing method (e.g., post-tensioning or pre-tensioning), the arrangement of fixed and free ends, the stressing apparatus deployed, and the quantification of applied forces, necessitating thorough compilation of:

(a) Post Tension Material with Modulus of Elasticity

(b) Profile of Tendons with Stressing and Dead ends

(c) Number of Strands

(d) Diameter and Area of Strands

(e) Ultimate and Yield Strengths of Strands

(f) Pulling Force / Jack Ratio

(g) Stressing Sequence and Records

(h) Actual Elongation Data Sheet

(i) Angular and Wobble friction coefficient of Strands

Executing stress assessments on the bridge span concurrent with the pre-stressing procedure, employing suitable instrumentation and methodologies, subsequently an in-depth examination to be conducted for the acquired stress measurements. Recording the initial readings of each strain gauge to be commenced before initiating the pre-stressing operation. Then log strain gauge readings to be taken continuously during the course of the pre-stressing operations, and optionally then the to be released. Comparative analysis to be conducted so as to quantify the stress variations throughout the entirety of the pre-stressing process. While executing the pre-stressing procedure stress assessments across the bridge span to be conducted employing suitable instrumentation and methodologies. Subsequently an exhaustive examination and presentation of the acquired stress measurements to be performed as stated below:

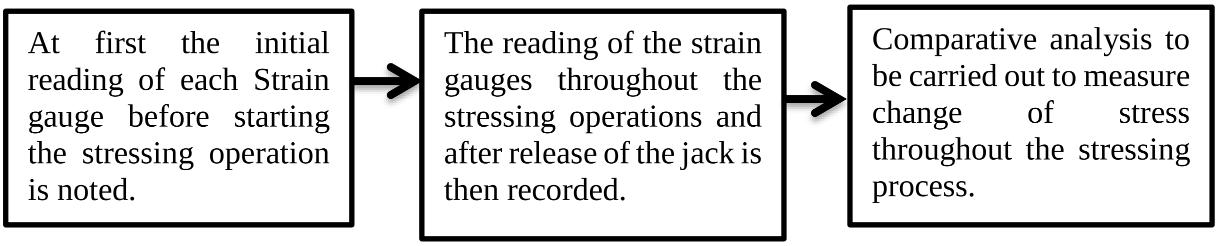

At first the initial reading of each Strain gauge before starting the stressing operation is noted.

The reading of the strain gauges throughout the stressing operations and after release of the jack is then recorded.

Comparative analysis to be carried out to measure change of stress throughout the stressing process.

The stress alteration pattern is contingent upon the stressing method employed, whether it is single-ended or double-ended. An examination must be conducted to derive the uplifting force of the tendon, subsequently facilitating the computation of the post-stressing uplift induced by the tendons. The subsequent procedure is to be employed to analyze the data set and construe the stress variation:

- From the strain gauges Frequency in hertz is being measured and noted.

- The frequency is being converted to micro strain as per the following formula:

,

$$\Delta\mu\varepsilon = \frac{(F_{current}^2 - F_{initial}^2) X\ Gauge\ Factor}{1000}$$

- Gauge factor as obtained from Calibration Certificate of the Strain Gauge is 3.967.

- The micro strain is then converted to strain (ε) after multiplying by 10^{-6}.

The subsequent stages involve determining the stress (N/mm²) through the multiplication of the modulus of elasticity of concrete. This modulus can be derived in accordance with the guidelines outlined in IS 456: 2000, wherein

$$E_c = 5000\sqrt{f_{ck}}$$ Where,

f_{ck} = Characteristic strength of the concrete.

4. Simulation using Computer Software

The computer model using ADAPT ABI [14] comprises a realistic representation of the bridge span, including the pre-stressing cables and surrounding concrete structure. The cables' material properties, geometry, and anchorage details are incorporated based on real-world data. Strain gauges are strategically placed along the cables' length to capture strain changes accurately. The simulation involves step-by-step loading of the cables, mimicking the actual stressing process. Here, 30 m long Bridge Girder has been considered as the test span. The girder is assumed to be straight in plan. Cross sections and typical Tendons are shown in figure 2. The material properties of pre-stressed cable bridge is given in Table 1 and details of tendons are given in table 2.

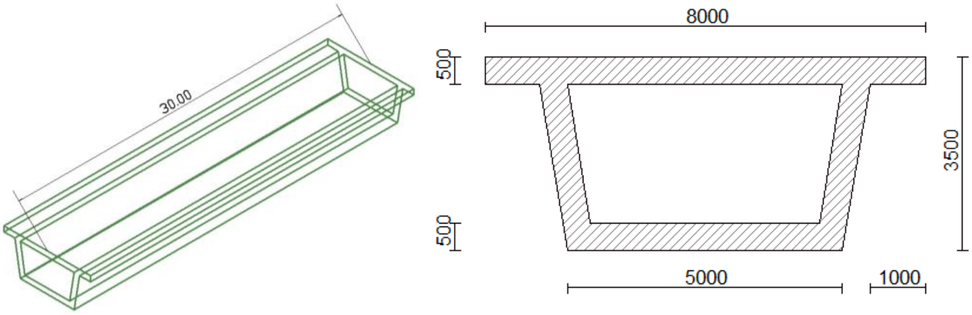

Fig. 2. Test Bridge Span and Cross Section

Table 1: Material properties of pre-stressed cable bridge

Properties of Bridge Section	
Depth of the Girder	3500 mm
Moment of Inertia	1.56 x 10^{13} mm^4
Cross Sectional Area	9.04 x 10^6 mm^2
Top fiber from Centroid	1,507.68 mm
Bottom fiber from Centroid	1,992.32 mm
Characteristics of material used in computer modelling	
Comprehensive Strength of the Concrete	
On 28th day	42.5 MPa
On Stressing Day (7th)	35.2 MPa
Properties of Reinforcement	
Modulus of Elasticity	2 x 10^5 MPa
Yield strength	500 MPa
Properties of Pre-stressing Material	
Modulus of Elasticity	2 x 10^5 MPa
Ultimate Stress	1860 MPa
Yield Stress	1700 MPa

Table 2: Details of tendons

Parameters	**Results**
Jacking Stress	75% of the Ultimate
Seating Loss	9 mm
Angular friction coefficient	0.25
Wobble friction coefficient	0.004 rad/m

Each parameter is sequentially manipulated to assess its individual impact on the Tendon Force. Table 3 illustrates the scenarios wherein Case 1 remains unaffected by the influences of all contributing factors. Conversely, Cases 2 through 5 encompasses singular variations in line with the specified conditions, while the other factors are maintained at their Case 1 levels. In Case 6, where all influencing factors are active, the stressing occurs from one end, while Case 7 involves stressing from both ends. In both instances, the assessment is conducted during the stressing phase but prior to jack release, denoting a Seating Loss of 0.0 mm.

Table 3: Typical Cases for Studying Effect of Individual Parameter

Case ID	**Parameters**
Case 1	● Jacking Stress is 100% of the Ultimate ● Seating Loss is 0.0 mm ● Angular friction coefficient is 0.0 ● Wobble friction coefficient is 0.0 rad/m
Case 2	● Jacking Stress is 75% of the Ultimate

Case ID	Parameters
	- Remaining Parameters are same as Case 1
Case 3	- Seating Loss is 9.0 mm - Remaining Parameters are same as Case 1
Case 4	- Angular friction coefficient is 0.25 - Remaining Parameters are same as Case 1
Case 5	- Wobble friction coefficient is 0.004 rad/m - Remaining Parameters are same as Case 1
Case 6	- Jacking Stress is 75% of the Ultimate - Stressing is done from one end - Angular friction coefficient is 0.25 - Wobble friction coefficient is 0.004 rad/m
Case 7	- Jacking Stress is 75% of the Ultimate - Stressing is done from both ends - Angular friction coefficient is 0.25 - Wobble friction coefficient is 0.004 rad/m
Case 8	- Seating Loss is 9.0 mm - Jacking Stress is 75% of the Ultimate - Stressing is done from one end - Angular friction coefficient is 0.25 - Wobble friction coefficient is 0.004 rad/m
Case 9	- Seating Loss is 9.0 mm - Jacking Stress is 75% of the Ultimate - Stressing is done from both ends - Angular friction coefficient is 0.25 - Wobble friction coefficient is 0.004 rad/m

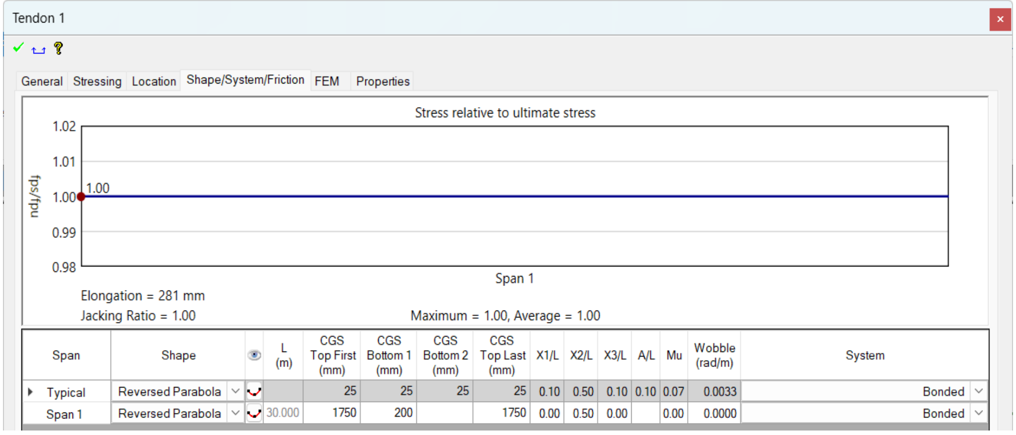

Elongation = 281 mm
Jacking Ratio = 1.00

Maximum = 1.00, Average = 1.00

Span	Shape		L (m)	CGS Top First (mm)	CGS Bottom 1 (mm)	CGS Bottom 2 (mm)	CGS Top Last (mm)	X1/L	X2/L	X3/L	A/L	Mu	Wobble (rad/m)	System
Typical	Reversed Parabola			25	25	25	25	0.10	0.50	0.10	0.10	0.07	0.0033	Bonded
Span 1	Reversed Parabola		30.000	1750	200		1750	0.00	0.50	0.00		0.00	0.0000	Bonded

Fig. 3 Tendon Force Diagram for Case 1 (100% throughout the length)

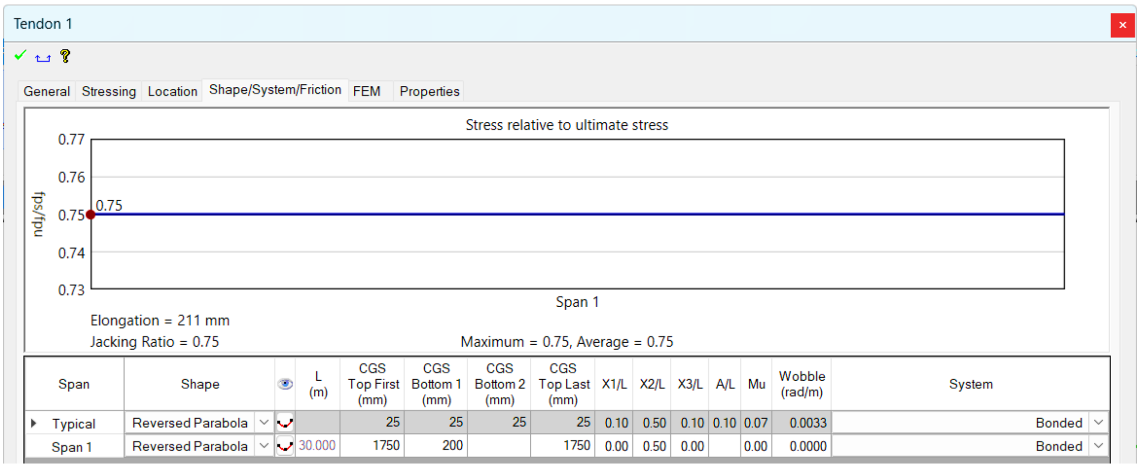

Elongation = 211 mm
Jacking Ratio = 0.75
Maximum = 0.75, Average = 0.75

Span	Shape	👁	L (m)	CGS Top First (mm)	CGS Bottom 1 (mm)	CGS Bottom 2 (mm)	CGS Top Last (mm)	X1/L	X2/L	X3/L	A/L	Mu	Wobble (rad/m)	System
Typical	Reversed Parabola			25	25	25	25	0.10	0.50	0.10	0.10	0.07	0.0033	Bonded
Span 1	Reversed Parabola		30.000	1750	200		1750	0.00	0.50	0.00		0.00	0.0000	Bonded

Fig. 4 Tendon Force Diagram for Case 2 (75% throughout the length)

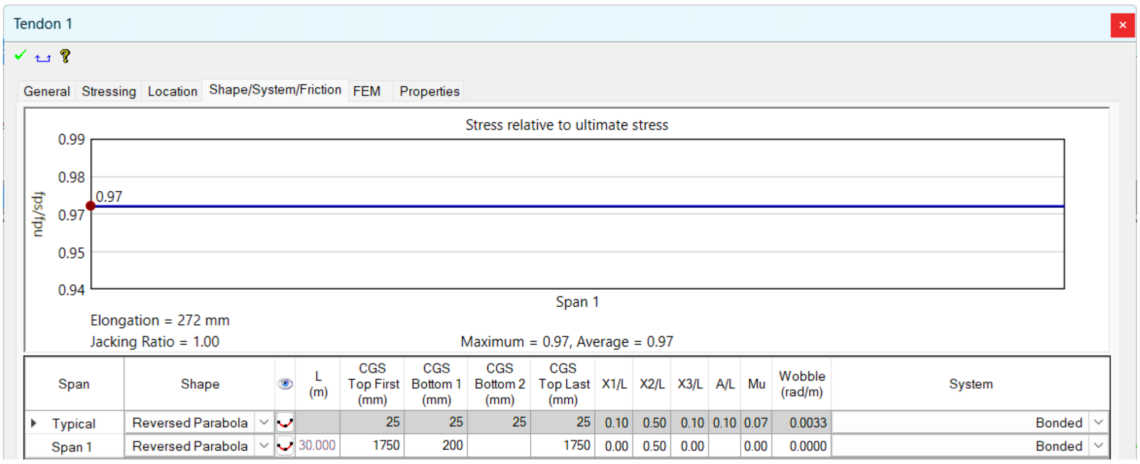

Elongation = 272 mm
Jacking Ratio = 1.00
Maximum = 0.97, Average = 0.97

Span	Shape	👁	L (m)	CGS Top First (mm)	CGS Bottom 1 (mm)	CGS Bottom 2 (mm)	CGS Top Last (mm)	X1/L	X2/L	X3/L	A/L	Mu	Wobble (rad/m)	System
Typical	Reversed Parabola			25	25	25	25	0.10	0.50	0.10	0.10	0.07	0.0033	Bonded
Span 1	Reversed Parabola		30.000	1750	200		1750	0.00	0.50	0.00		0.00	0.0000	Bonded

Fig. 5 Tendon Force Diagram for Case 3 (97% throughout the length)

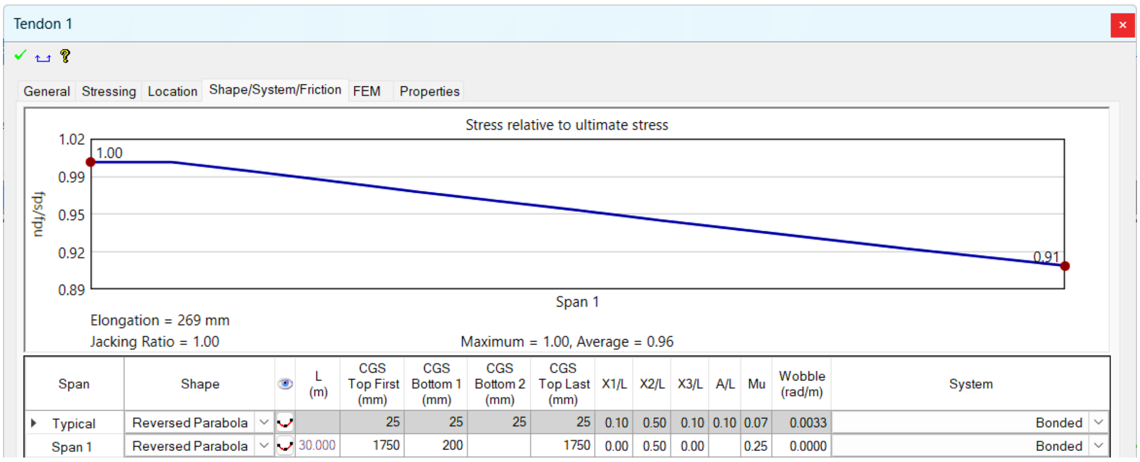

Elongation = 269 mm
Jacking Ratio = 1.00
Maximum = 1.00, Average = 0.96

Span	Shape	👁	L (m)	CGS Top First (mm)	CGS Bottom 1 (mm)	CGS Bottom 2 (mm)	CGS Top Last (mm)	X1/L	X2/L	X3/L	A/L	Mu	Wobble (rad/m)	System
Typical	Reversed Parabola			25	25	25	25	0.10	0.50	0.10	0.10	0.07	0.0033	Bonded
Span 1	Reversed Parabola		30.000	1750	200		1750	0.00	0.50	0.00		0.25	0.0000	Bonded

Fig. 6 Tendon Force Diagram for Case 4 (100% throughout the length)

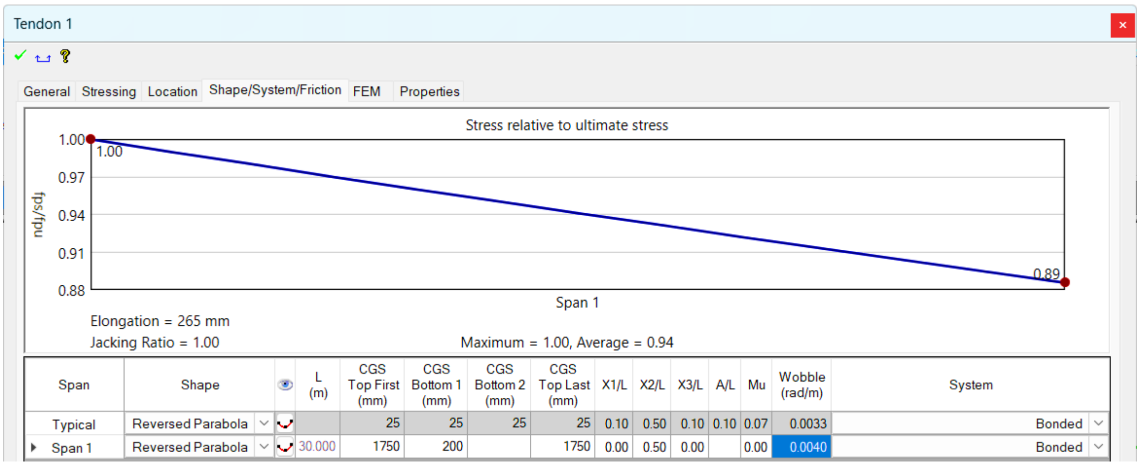

Elongation = 265 mm
Jacking Ratio = 1.00

Maximum = 1.00, Average = 0.94

Span	Shape		L (m)	CGS Top First (mm)	CGS Bottom 1 (mm)	CGS Bottom 2 (mm)	CGS Top Last (mm)	X1/L	X2/L	X3/L	A/L	Mu	Wobble (rad/m)	System
Typical	Reversed Parabola			25	25	25	25	0.10	0.50	0.10	0.10	0.07	0.0033	Bonded
Span 1	Reversed Parabola		30.000	1750	200		1750	0.00	0.50	0.00		0.00	0.0040	Bonded

Fig.7 Tendon Force Diagram for Case 5 (100% at stressing end and linearly declined to 89% on dead end)

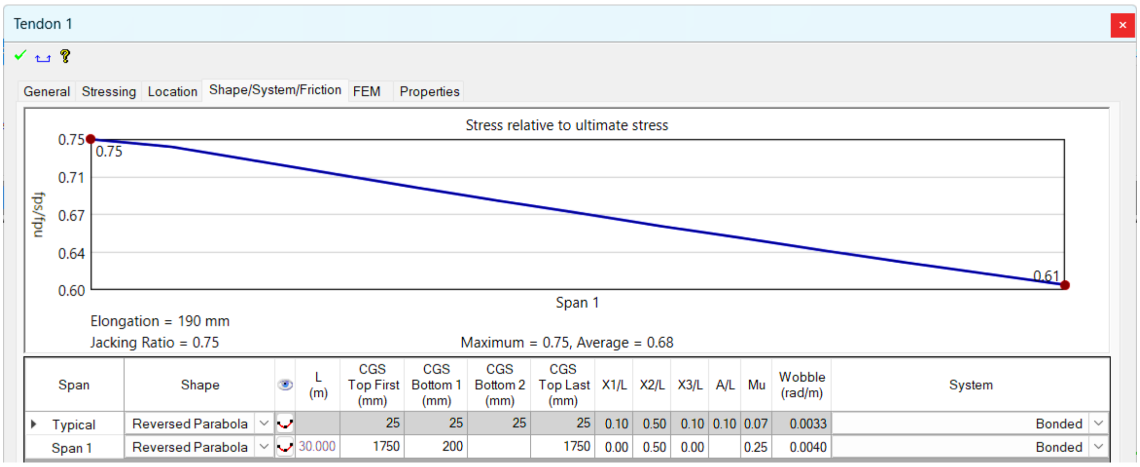

Elongation = 190 mm
Jacking Ratio = 0.75

Maximum = 0.75, Average = 0.68

Span	Shape		L (m)	CGS Top First (mm)	CGS Bottom 1 (mm)	CGS Bottom 2 (mm)	CGS Top Last (mm)	X1/L	X2/L	X3/L	A/L	Mu	Wobble (rad/m)	System
Typical	Reversed Parabola			25	25	25	25	0.10	0.50	0.10	0.10	0.07	0.0033	Bonded
Span 1	Reversed Parabola		30.000	1750	200		1750	0.00	0.50	0.00		0.25	0.0040	Bonded

Fig. 8 Tendon Force Diagram for Case 6 (75% at stressing end and linearly declined to 61% on dead end)

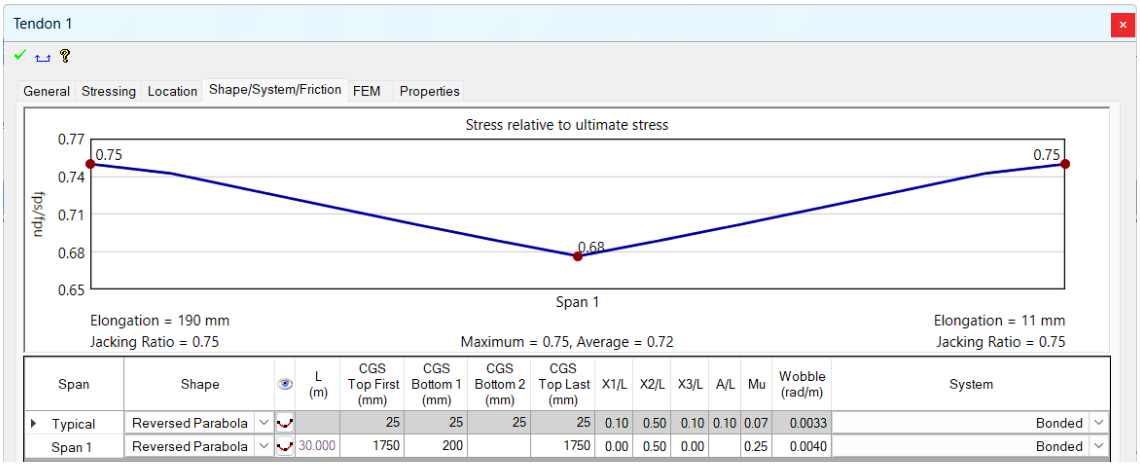

Elongation = 190 mm
Jacking Ratio = 0.75

Maximum = 0.75, Average = 0.72

Elongation = 11 mm
Jacking Ratio = 0.75

Span	Shape		L (m)	CGS Top First (mm)	CGS Bottom 1 (mm)	CGS Bottom 2 (mm)	CGS Top Last (mm)	X1/L	X2/L	X3/L	A/L	Mu	Wobble (rad/m)	System
Typical	Reversed Parabola			25	25	25	25	0.10	0.50	0.10	0.10	0.07	0.0033	Bonded
Span 1	Reversed Parabola		30.000	1750	200		1750	0.00	0.50	0.00		0.25	0.0040	Bonded

Fig. 9 Tendon Force Diagram for Case 7 (75% at stressing end, linearly declined to 68% at the middle and again increasing to 75%)

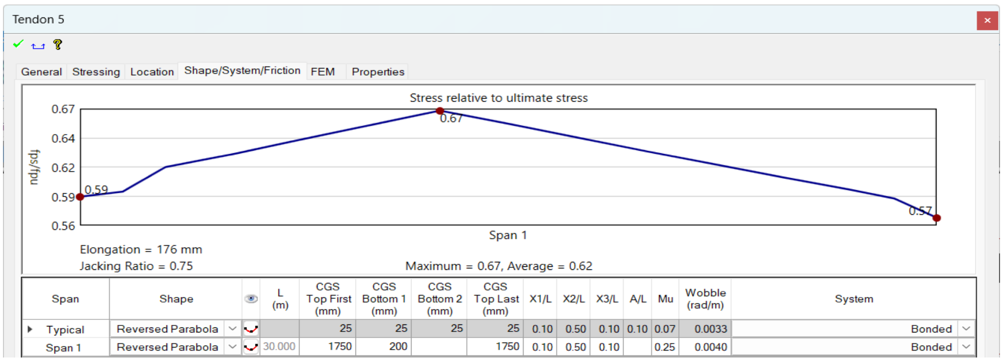

Elongation = 176 mm
Jacking Ratio = 0.75
Maximum = 0.67, Average = 0.62

Span	Shape		L (m)	CGS Top First (mm)	CGS Bottom 1 (mm)	CGS Bottom 2 (mm)	CGS Top Last (mm)	X1/L	X2/L	X3/L	A/L	Mu	Wobble (rad/m)	System
Typical	Reversed Parabola			25	25	25	25	0.10	0.50	0.10	0.10	0.07	0.0033	Bonded
Span 1	Reversed Parabola		30.000	1750	200		1750	0.10	0.50	0.10		0.25	0.0040	Bonded

Fig. 10 Tendon Force Diagram for Case 8 (59% at stressing end, incrementally going up to 67% near middle and coming down to 57% at dead end)

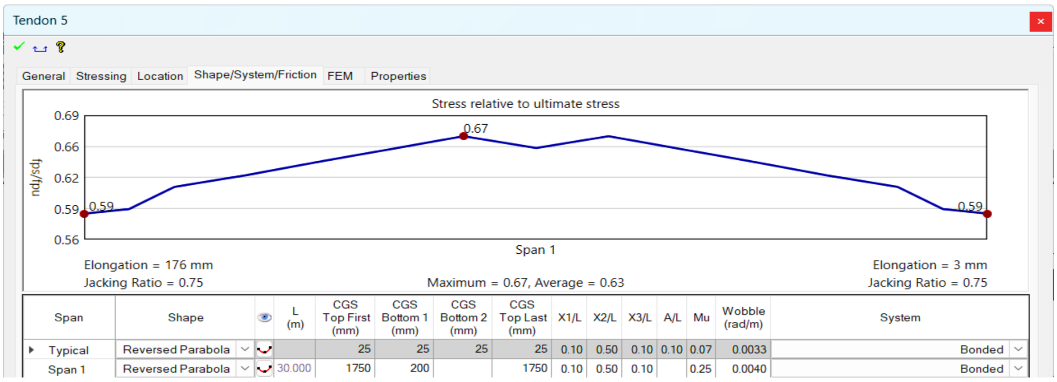

Elongation = 176 mm
Jacking Ratio = 0.75
Maximum = 0.67, Average = 0.63
Elongation = 3 mm
Jacking Ratio = 0.75

Span	Shape		L (m)	CGS Top First (mm)	CGS Bottom 1 (mm)	CGS Bottom 2 (mm)	CGS Top Last (mm)	X1/L	X2/L	X3/L	A/L	Mu	Wobble (rad/m)	System
Typical	Reversed Parabola			25	25	25	25	0.10	0.50	0.10	0.10	0.07	0.0033	Bonded
Span 1	Reversed Parabola		30.000	1750	200		1750	0.10	0.50	0.10		0.25	0.0040	Bonded

Fig. 11 Tendon Force Diagram for Case 9 (59% at stressing end, going up to 67% near middle and coming down to 59% at second stressing end)

Table 4: Typical Cases for Studying Effect of Individual Parameter

Case ID	Tendon Force	Loss of Force
Case 1	1.00	Zero
Case 2	0.75	25% through-out
Case 3	0.98	2% through-out
Case 4	1.0 to 0.91	0% at stressing end to 9% at dead end
Case 5	1.0 to 0.89	0% at stressing end to 11% at dead end
Case 6	0.75 to 0.61	0% at stressing end to 14% at dead end
Case 7	0.75 to 0.68 to 0.75	0% at both ends and 9% at the middle
Case 8	0.59 to 0.67 to 0.57	16% at stressing end, 18% at dead end and 8% at the middle
Case 9	0.59 to 0.67 to 0.59	16% at both ends and 8% at the Middle

During the process of stressing, the upward deflection can be determined by calculating the precise value using the specific Tendon Profile and Stressing sequence (Ref Table 5 and Figure 13).

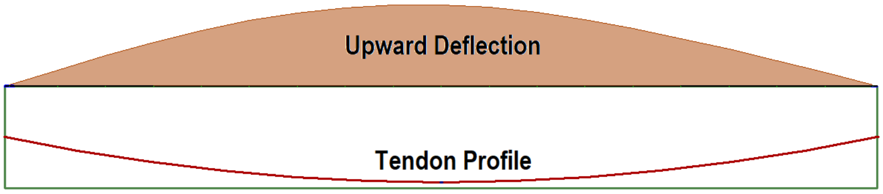

Fig. 12 Upward Deflection for Stressing of Tendons

In cases where an estimated Tendon Profile is considered characterized by a drape length of 1.55m (1.75m – 0.2m), the projected upward deflection values for Tendon Stressing are provided in the subsequent table.

Table 5: Anticipated Upward Deflection

Location ⇒	**at L/4 (mm)**	**at 2L/4 = L/2 (mm)**	**at 3L/4 (mm)**
Single end Stressing			
For each 12.7 mm Strand	0.04641	0.06480	0.04615
For each 15.2 mm Strand	0.06536	0.09126	0.06499
Both end Stressing			
For each 12.7 mm Strand	0.04961	0.06994	0.05048
For each 15.2 mm Strand	0.06987	0.09848	0.07108

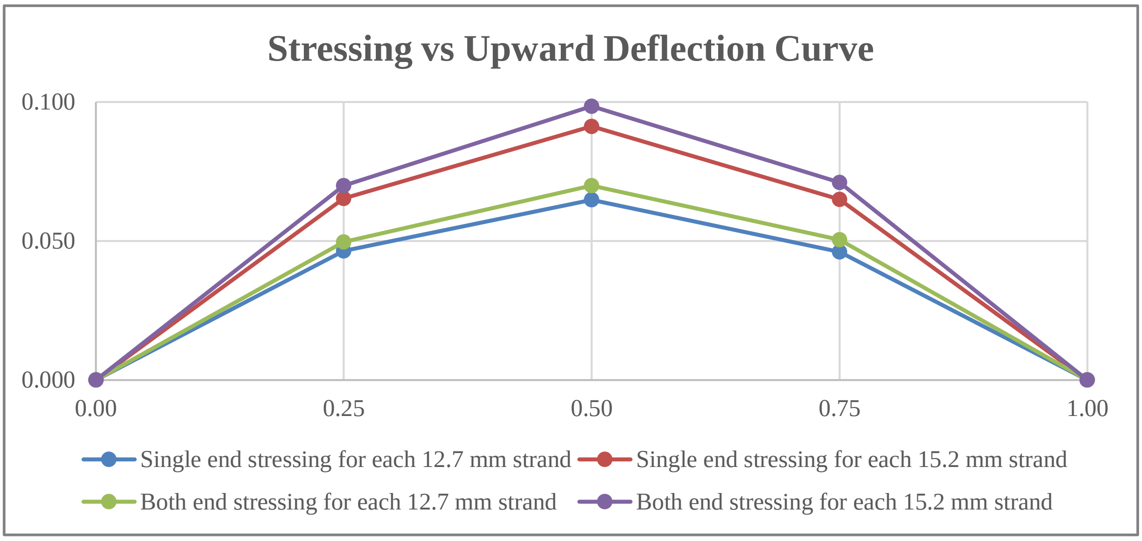

Fig.13 Stressing vs Upward Deflection Curve

Given that the assessment pertains to the stressing phase, the influence of Creep and Shrinkage has been omitted from consideration. Nonetheless, if Deflection or Strain measurements are taken after a temporal interval, it becomes imperative to integrate these effects into the adjustment of field data.

5. Conclusion

The influence of friction coefficients (including both friction and wobble effects) on the applied tendon force during the stressing process is readily apparent. Additionally, the configuration of the stressing ends plays a crucial role in determining the stress increment pattern along the tendon. In the scenario of single end stressing and from figure 3 to figure 11, it becomes evident that the stress alteration experiences a reduction of 3.5% at every interval of L/4 length. As the area of 15.2 mm strands are 40.5% more than 12.7 mm strand, the magnitude of upward deflection caused at each location for each condition is also having same impact. Otherwise for both end stressing for both end stressing the magnitude of deflections are 6.90%, 7.92% and 9.38% more respectively at L/4, L/2 and 3L/4 locations for same type of tendons.

6. Future Scope of Work

Future research work could focus on validating the simulation results through experimental testing and investigating the long-term effects of stress redistribution on the performance of pre-stressed concrete bridges.

References

[1] Omid Khandel, Mohamed Soliman, Royce W. Floyd & Cameron D. Murray, “Performance assessment of prestressed concrete bridge girders using fiber optic sensors and artificial neural networks”, *Structure and Infrastructure Engineering*, Volume 17, 2021 - Issue 5 (2020)

[2] Helder Sousa, Filipe Cavadas, António Henriques, João Bento, Joaquim Figueiras, “Bridge deflection evaluation using strain and rotation measurements”, *Smart Structures & Systems*, Vol 11, pages 365–386 (2013)

[3] Sreeshylam, Ravisankar, S. Parivallal, K. and Sridhar, “Condition monitoring of prestressed concrete structures using vibrating wire sensors”, *International Journal of COMADEM*, 11(3):46-54 (2008)

[4] Wei-Hua Hu, Samir Said, Jun Teng, “Continuous dynamic monitoring of a prestressed concrete bridge based on strain, inclination and crack measurements over a 14-year span”, *Structural Health Monitoring*, Vol 17, Issue 5 (2017)

[5] Wei Sun, Jun Du, Qiang Wang, Li Sun, “Multi point monitoring method of prestressed tendon based on distributed sensors”, *Journal of Physics: Conference Series*, 2093 (2021) 012042 (2021)

[6] Junhwa Lee a, Seunghoo Jeong b, Hyunjun Kim c, Kyoung Chan Lee d, Sung-Han Sim, “Comparative study of long-term displacement measurement methods – Focusing on a Pre-stressed concrete bridge under construction”, *Measurement*, Vol 201, 111691 (2022)

[7] Bin Zhou, Xiang Zhang, Yanguang Xue, “Stress Monitoring for Cantilever Construction of Concrete Continuous Bridge with Variable Cross-section, *Advances in Engineering Research*, Vol 129, 6th International Conference on Energy, Environment and Sustainable Development (ICEESD 2017)

[8] Ammar Zalt, “Health Monitoring of Concrete Bridges Utilizing Sensor Technology” *PhD Thesis work*, Western Michigan University Kalamazoo, Michigan (2007)

[9] Indian Standard Specification, IS 456, “Plain and Reinforced Concrete: Code of Practice (2000).

[10] R. Manisekar, “Monitoring the Prestress in prestressed concrete bridges- some suggestion”, Journal of Indian Road Congress, April-June 2020.

[11] C. Roberts-Wollmann, J. Arréllaga, M. Kreger, “Field measurement of prestress losses in external tendons”, ACI Structural Journal (1996)